American Mineralogist, Volume 81, pages 1270–1276, 1996

Description and crystal structure of fianelite, $Mn_2V(V,As)O_7 \cdot 2H_2O$, a new mineral from Fianel, Val Ferrera, Graubünden, Switzerland

JOËL BRUGGER AND PETER BERLEPSCH

Mineralogisch-Petrographisches Institut, Bernoullistrasse 30, CH-4056 Basel, Switzerland

ABSTRACT

Fianelite occurs in iron and manganese ores at Fianel, a small mine in Val Ferrera, Graubünden, Switzerland. It is associated with quartz, aegirine, and limonite in thin open fractures crosscutting quartz + rhodonite + kutnohorite + palenzonaite ± aegirine ± parsettensite ± saneroite ± pyrobelonite veinlets. Only a small amount of very minute, tabular, (010)-flattened fianelite crystals have been collected. Fianelite, with ideal formula $Mn_2V(V,As)O_7 \cdot 2H_2O$, crystallizes in the $P2_1/n$ space group with $a = 7.809(2)$, $b = 14.554(4)$, $c = 6.705(4)$ Å and $\beta = 93.27(3)°$. The strongest lines in the X-ray powder pattern are $d_{022,230} = 3.039$, $d_{120} = 5.32$, $d_{231} = 2.721$, and $d_{163,36\bar{2}} = 1.593$ Å. The orange-red mineral is transparent; its optical sign is unknown, and $2V$ is small. Fianelite shows a strong pleochroism from yellow to red. Microprobe analyses revealed a partial substitution of As for V, leading to the empirical formula $Mn_{1.98}(V_{1.57}As_{0.44}Si_{0.01})O_7 \cdot 2H_2O$. The crystal structure of fianelite, refined to $R = 0.058$, consists of Mn in octahedral chains bound together by pairs of V in tetrahedra. Among the two V positions, only one hosts As. H is present in H_2O groups belonging to the octahedra and occupying channels extending through the structure along [001]. No mineral having a chemical formula with the same atomic proportions as fianelite shows similar structural features.

INTRODUCTION

Systematic examination of the geology and mineralogy of several small iron and iron-manganese deposits embedded in the Triassic sediments that occur on top of the Suretta basement nappe in the eastern Swiss Alps led to the discovery of a new manganese vanadate. Its chemical features are related to other natural compounds, such as reppiaite [$Mn_5^{2+}(VO_4)_2(OH)_4$; Basso et al. 1992], variscite ($AlPO_4 \cdot 2H_2O$; Kniep et al. 1977), fluckite [$CaMn(AsO_3OH)_2 \cdot 2H_2O$; Bari et al. 1980, Catti et al. 1980], and the haidingerite-group minerals, e.g., krautite [$Mn(AsO_3OH) \cdot H_2O$; Fontan et al. 1975, Catti and Franchini-Angela 1979, Beneke and Lagaly 1981] and haidingerite [$Ca(AsO_3OH) \cdot H_2O$; Cassien et al. 1966, Calleri and Ferraris 1967].

The new mineral was named "fianelite" for the type locality, Fianel, a mine in Val Ferrera, Graubünden, Switzerland. The mineral and the name have been approved by the International Mineralogical Association Commission on New Minerals and Mineral Names. Type material is deposited in the collection of the Naturhistorisches Museum, Abteilung für Mineralogie, Basel, Switzerland.

OCCURRENCE AND GENETIC ENVIRONMENT

The Suretta nappe (Pennine realm of the eastern part of the Central Alps) belongs to the easternmost members of the paleogeographic "Briançonnais domain," characterized by shallow-water sedimentation during the Mesozoic (Trümpy 1980). The Suretta nappe consists of three principal lithostratigraphic units: (1) a pre-Variscan basement containing various lithologies, (2) the "Roffnaporphyr" (late-Variscan granitic complex), and (3) a Mesozoic cover. The latter consists of basal quartzites followed by dolomitic and calcitic marbles attributed mainly to the Triassic. However, recent structural and lithostratigraphic work (Baudin et al. 1995) points to greater complexity in the cover of the Suretta nappe: The Mesozoic series seems to be more complete, and there is evidence of nappe tectonics within the cover, which was formerly considered to be autochtonous.

The dolomitic marbles (Triassic) contain numerous small stratabound iron and iron-manganese deposits. All the lithologies, including the deposits, underwent polyphase Alpine metamorphism with a climax under greenschist-facies conditions (Schmid et al. 1990; Schreurs 1991).

Our systematic study of the carbonate-hosted mineralization around the Suretta nappe led to a new petrographic description of the manganoan ores and to the discovery of a general V-As content associated with these ores. The Fianel deposit is remarkable because of the variety of its ores, as originally emphasized by Stucky (1960). The lenticular ore body (60 m long × 50 m wide × 12 m in maximal height) consists of (1) an iron oxide ore (hematite + quartz ± strontian barite ± fluorapatite), (2) an iron silicate ore (aegirine ± quartz ± strontian

0003–004X/96/0910–1270$05.00

TABLE 1. Optical and other physical properties of fianelite

$2V_{obs} < 10°$
Optical sign: unknown
Pleochroism on (010): strong, yellow to red
$n_{red} = 1.82(2)$; $n_{yellow} = 1.82(2)$ (at 25 °C, for 589 nm)
Orientation of the indicatrix: angle between n_{yellow} and *a* axis = 16(1)°; the optical axes lie near n_{yellow}
Density (meas.): 3.21(1) g/cm³ (heavy liquids)
Density (calc. for the formula $Mn_2V(V_{0.62}As_{0.38})O_7 \cdot 2H_2O$): 3.217(2) g/cm³
Color: orange-red
Streak: orange
Luster: vitreous
Transparent, nonfluorescent
Cleavage: good parallel {001}? and {100}?
Hardness [VHN(15) on (010) face]: mean 86.5 kg/mm², range 84–89 kg/mm²
Twinning: not observed; common intergrowths parallel [100]

FIGURE 1. SEM photo of fianelite crystals. Notice the strong striation parallel to the *a* axis. Field of view is ~0.25 mm.

barite), and (3) a complex iron-manganese ore (quartz + braunite + jacobsite + hematite + rhodonite + tephroite + rhodochrosite + kutnohorite + calderite + spessartine ± fluorapatite ± strontian barite ± barylite ± medaite. . . .)

Stratabound medaite-rich ores (up to 3 vol% medaite) occur inside the iron and manganese ores as lenses measuring up to 20 cm thick and 2 m in lateral extension. Medaite forms small (<200 μm) xenomorphic grains lying in the main schistosity and giving the rock a typical red color.

The ores are crosscut by several generations of centimeter-wide veinlets with mineral assemblages that depend on the embedding rock. Within the medaite-rich rocks, these veinlets contain quartz, rhodonite, kutnohorite, aegirine, parsettensite, and several rare V minerals: palenzonaite, $NaCa_2Mn_2(VO_4)_3$; saneroite, $Na_2Mn_{10}VSi_{11}O_{34}(OH)_4$; and pyrobelonite, $PbMnVO_4(OH)$. These veins are in turn crosscut by thin open fractures (<1 mm) containing quartz, aegirine, iron hydroxide-oxides (limonite), and tiny orange-red crystals of fianelite.

Fianelite represents the last generation of vanadate crystallization at Fianel. Medaite grew syntectonically within the main schistosity during the first crystallization stage (prograde metamorphic stage). During the second stage (retrograde metamorphic stage), V from the medaite-rich layers was mobilized into palenzonaite-bearing veinlets crosscutting the main foliation. These features make Fianel mineralogically very similar to other Alpine metamorphic Mn deposits such as (1) Falotta, Graubünden, Switzerland (Geiger 1948), which is the type locality for geigerite $[Mn_5(AsO_4)_2(AsO_3OH)_2 \cdot 10H_2O$; Graeser et al. 1989] and grischunite $[NaCa_2Mn_5Fe(AsO_4)_6 \cdot 2H_2O$; Graeser et al. 1984]; and (2) Val Graveglia, Northern Apennines, Italy (Cortesogno et al. 1979), which is the type locality for palenzonaite (Basso 1987), saneroite (Lucchetti et al. 1981), and reppiaite (Basso et al. 1992). These other deposits, however, are embedded in metaradiolarites representing the first sediments on ocean-floor basalts, whereas the Fianel deposit occurs in platform carbonates sedimented over a continental basement. The radiolarite-hosted deposits are of synsedimentary exhalative origin. The similarity of the geochemistry of the radiolarite-hosted deposits with that of Fianel suggests a similar exhalative origin for the latter deposit. The occurrence of ore fragments within Mesozoic breccia near Fianel further supports such a syngenetic model.

OPTICAL AND OTHER PHYSICAL PROPERTIES

The optical and other physical properties of fianelite are summarized in Table 1. The mineral occurs mostly in polycrystalline crusts (<100 μm thick, up to 2.5 mm in diameter). The rare single crystals (up to 0.2 mm) display a platy habit with a well-developed {010} pinacoid and are deeply striated parallel to the *a* axis. The crystals are sometimes grouped in rosettes, and intergrowths of individuals parallel to the *a* axis are common; indeed, some macroscopically homogenous crystals appear to comprise numerous tiny prismatic individuals lying parallel to the *a* axis (Fig. 1). One crystal could be measured with an optical goniometer (Fig. 2). Under the scanning electron microscope (SEM), rare isolated crystals displaying {100}, {001}, and possibly {041} were observed.

Under the polarizing microscope, fianelite crystals are generally transparent, but some difficulties were encountered during the optical measurements owing to morphology, size, and amount of material. For example, the platy habit and the strong absorption prevented measurement of the refractive index parallel to the *a* axis (immersion method). For the same reason, only a poor conoscopic image could be obtained, precluding the determination of the optical sign. Using the Gladstone-Dale relationship (Mandarino 1976), and depending on the As content, a mean refractive index between 1.83 and 1.87 was calculated. The two refractive indices on the face (010) were measured on two separate crystals; both indices lie between the 1.800(5) and 1.840(5) immersion liquids.

Microhardness was measured by a Leitz Durimet microscope on the (010) face only. The VHN values obtained correspond to a Mohs hardness of approximately 3.

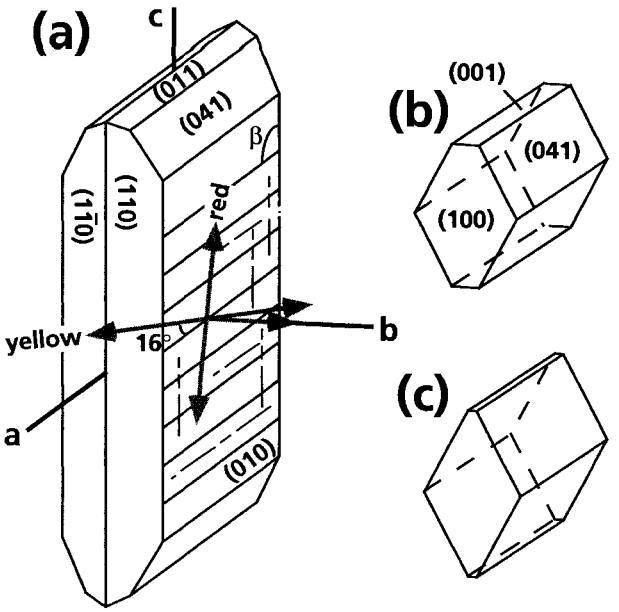

FIGURE 2. Morphology of fianelite crystals. (**a**) Ideal drawing of a fianelite crystal measured on an optical goniometer (longest axis = 0.2 mm). Dashed lines indicate traces of the cleavage on the (010) face. (**b** and **c**) Ideal drawings of two tiny fianelite crystals that were located on the (010) face of the crystal shown in **a**.

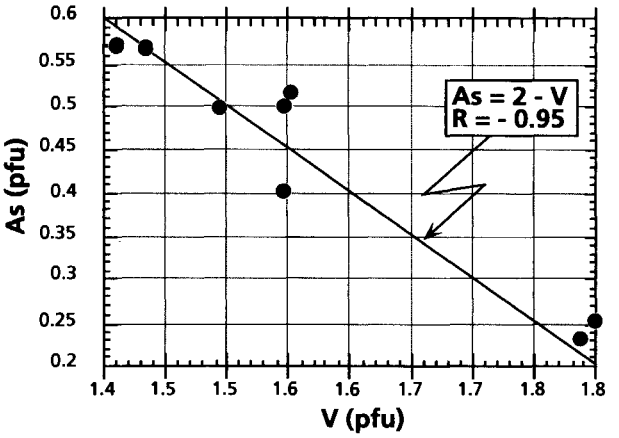

FIGURE 3. Plot of the number of As atoms pfu vs. V atoms pfu from microprobe analyses of fianelite, normalized on the basis of four cations.

CHEMICAL COMPOSITION

The results of the chemical analyses are summarized in Table 2. Eight analyses were performed on three crystals with the use of a JEOL JXA-8600 electron microprobe (EMP) operated at 15 kV, 10 nA, and a surface-scanning area of 15 μm^2 with a point-focused beam. The following standards, X-ray lines, and detector crystals were used for the calibration: spessartine (Mn$K\alpha$, LiF), adamite (As$L\alpha$, TAP), V_2O_5 (V$K\alpha$, LiF), and albite (Si$K\alpha$, TAP). P_2O_5, Na_2O, CaO, and MgO were measured and are all below 0.05 wt%. Using WDS scans, no additional element with atomic number ≥9 was detected. The H_2O content could not be determined by an analytical method owing to paucity of material. However, if the weight percent of H_2O calculated from the H_2O content deduced from the crystal-structure analysis is added, a satisfactory analytical total is obtained. The empirical formula (on the basis of four cations, mean of eight analyses on three grains) is $Mn_{1.98}(V_{1.57}As_{0.44}Si_{0.01})O_7 \cdot 2H_2O$. A good negative correlation ($R = -0.95$) between As and V indicates considerable substitution of V by As (Fig. 3). Among the three analyzed grains, two are homogenous [0.57 and 0.51

TABLE 2. Chemical data for fianelite (eight analyses on three grains)

Oxide	wt%	Range	σ
V_2O_5	38.23	33.15–43.89	4.03
As_2O_5	13.57	7.23–17.05	4.00
SiO_2	0.12	<0.04–0.25	0.02
MnO	37.49	36.70–39.50	0.93
Total	89.41	86.96–92.91	2.31
H_2O_{calc}*	9.64		
Total	99.05		

* H_2O calculated on the basis of 2 H_2O pfu, as determined by the crystal-structure analysis.

TABLE 3. X-ray powder diffraction data for fianelite (*d* in Å)

d_{meas}	Int*	d_{calc}**	*hkl*
7.28	40	7.277	020
6.87	20	6.872	110
6.06	30	6.082	011
5.32	80	5.320	120
4.92	30	4.927	021
		4.921	11$\bar{1}$
4.68	30	4.679	111
4.12	20	4.119	130
3.928	40	3.928	031
3.436	50	3.436	220
3.361	20	3.362	21$\bar{1}$
3.259	50	3.262	012
3.039	100	3.041	022
		3.039	230
2.785	20	2.785	122
2.721	60	2.722	231
2.631	20	2.637	13$\bar{2}$
2.573	50	2.573	21$\bar{2}$
2.444	50	2.447	320
2.336	40	2.332	250
2.199	20	2.200	16$\bar{1}$
2.137	10	2.135	331
		2.133	023
1.989	10	1.990	341
1.964	5	1.964	062
1.882	<5	1.884	252
1.838	10	1.841	351
1.825	10	1.828	143
1.708	40	1.707	181
1.593	60	1.594	163
		1.593	36$\bar{2}$

* Intensities assigned by visual estimate.

** Calculated on the basis of the cell parameters listed in Table. 4. Indices were chosen using theoretical intensities calculated by the program LAZY PULVERIX (Yvon et al. 1977).

TABLE 4. Structure-analysis data for fianelite

Ideal formula	$Mn_2V(V,As)O_7 \cdot 2H_2O$
Formula from structure refinement	$Mn_2V(V_{0.62}As_{0.38})O_7 \cdot 2H_2O$
Space group	$P2_1/n$
a	7.809(2) Å
b	14.554(4) Å
c	6.705(4) Å
β	93.27(3)°
V	760.8(5) Å^3
Z	4
Instrumentation	ENRAF NONIUS CAD4
Rad./mon.	Cu/graphite
Scan technique	ω-2θ
Index range	$0 < h < 8$, $-18 < k < 0$, $-9 < l < 9$
No. of refl.	1776 (total)
Absorption-correction methods	ψ scan and DIFABS
μ	4.54 mm^{-1}
Min./max. correction	0.51/1.00
Final merging R factor	0.049
No. of used refl.	706 [$I > 3\sigma_I$]
Final R and R_w	0.058 and 0.046

As per formula unit (pfu)] and the third shows an internal zonation from 0.23 to 0.57 As pfu.

X-RAY SINGLE-CRYSTAL AND POWDER DATA

Preliminary single-crystal studies, using Weissenberg and precession methods, determined the unit cell and space group and helped to select a crystal of sufficient quality for the structure determination.

The X-ray powder diffraction pattern was obtained with a Gandolfi camera (114.6 mm in diameter) using Mn-filtered Fe$K\alpha$ radiation (λ = 1.93728 Å). The X-ray powder diffraction data for fianelite are listed in Table 3. Relative intensities of the reflections were assigned by visual estimate.

The unit-cell parameters were derived by least-squares refinement using two data sets obtained from different crystals: (1) CAD4 data and (2) powder diagram. The two data sets show significantly different results for only the β cell parameter: β = 93.27(3)° for CAD4 data and β = 93.13(3)° for powder data. Considering the large range of V vs. As substitution, the agreement between the two cell parameter sets is excellent. The cell parameters reported in Table 4 are for the single-crystal data.

STRUCTURE SOLUTION AND REFINEMENT

The X-ray data were collected from a short prismatic crystal, about 0.035 × 0.060 × 0.065 mm, with the use of an Enraf-Nonius CAD4 automatic single-crystal diffractometer with Kappa geometry. The lattice parameters were determined and refined, using 24 reflections within the angular range $12.8° < 2\theta < 53.6°$. Diffraction intensities were measured in the ω-2θ scan mode for $5.58° < 2\theta < 156°$, using graphite-monochromated Cu$K\alpha$ radiation (λ = 1.54178 Å). Data reduction included background and Lorentz-polarization corrections. The data were empirically corrected for absorption using ψ scans. The space group $P2_1/n$ was derived on the basis of the following systematic extinctions: $h0l$, $h + l \neq 2n + 1$; $0k0$, $k \neq 2n + 1$; $h00$, $h \neq 2n + 1$; and $00l$, $l \neq 2n + 1$.

Direct methods were successfully applied using the program SIR92 (Altomare et al. 1994) to locate all Mn, V, and O sites (13, assuming all positions were fully occupied). Least-squares refinement was performed using the program CRYSTALS (Watkin et al. 1985), assigning Chebychev weighting to the reflections (Carruthers and Watkin 1979). The observed structure factors are listed in Table 5.[1]

From the chemical analysis the total occupancy of the two Mn sites was fixed. Later, the occupancy of V vs. As in the two tetrahedral sites was refined separately, keeping the sum of V + As = 1. The scale factor, coordinates, and displacement parameters were simultaneously derived during the last cycle of refinement, which converged at R = 0.081, R_w = 0.096.

The high R_{merge} (ψ scans) value of 0.162 and the relatively poor R/R_w values were not satisfactory. It was assumed that the empirical correction for absorption (using ψ scans) was incomplete. By reprocessing the data using DIFABS (Walker and Stuart 1983) the R_{merge} value dropped to 0.049. Further refinement of the full matrix converged at R = 0.058, R_w = 0.046. Experimental details

[1] A copy of Table 5 may be ordered as Document AM-96-626 from the Business Office, Mineralogical Society of America, 1015 Eighteenth Street NW, Suite 601, Washington, DC 20036, U.S.A. Please remit $5.00 in advance for the microfiche.

TABLE 6. Fractional atomic coordinates and displacement parameters for fianelite

Atom	x/a	y/b	z/c	U_{iso}	U_{11}	U_{22}	U_{33}	U_{23}	U_{13}	U_{12}
Mn1	0.3987(3)	0.3846(1)	0.2378(4)	0.0118(4)	0.013(1)	0.0109(9)	0.012(1)	0.0005(9)	0.000(1)	0.0013(9)
Mn2	0.6200(3)	0.2475(2)	0.9615(3)	0.0131(4)	0.010(1)	0.0152(9)	0.016(1)	−0.001(1)	−0.001(1)	0.002(1)
V1	0.3285(3)	0.4211(1)	0.7458(4)	0.0088(4)	0.010(1)	0.0099(9)	0.007(1)	0.0007(9)	0.0007(9)	−0.0003(9)
V2*	0.0403(3)	0.3176(1)	0.9497(3)	0.0119(4)	0.012(1)	0.0135(8)	0.0104(9)	−0.0008(8)	0.0001(8)	−0.0006(8)
O1	0.165(1)	0.2928(6)	0.158(2)	0.014(2)	0.023(5)	0.019(4)	0.012(4)	0.002(4)	−0.012(4)	−0.004(4)
O2	0.058(1)	0.2360(6)	0.775(1)	0.012(2)	0.019(5)	0.010(4)	0.012(4)	−0.002(3)	0.003(4)	0.005(3)
O3	0.115(1)	0.4204(7)	0.848(2)	0.008(2)	0.003(4)	0.024(4)	0.025(5)	−0.005(4)	0.005(4)	−0.007(4)
O4	0.387(1)	0.5286(6)	0.706(2)	0.016(2)	0.025(5)	0.007(4)	0.026(5)	0.000(4)	−0.008(4)	−0.002(4)
O5	−0.164(1)	0.3394(6)	0.001(2)	0.018(2)	0.025(5)	0.011(4)	0.024(5)	0.001(4)	0.000(4)	0.006(4)
O6	0.458(1)	0.3674(7)	0.924(1)	0.013(2)	0.025(5)	0.021(4)	0.011(4)	−0.005(4)	0.011(4)	0.002(4)
O7	0.314(1)	0.3597(7)	0.529(1)	0.019(2)	0.025(5)	0.023(5)	0.015(5)	0.005(4)	0.007(4)	0.003(4)
W1	0.231(2)	0.5068(7)	0.236(2)	0.022(2)	0.027(6)	0.019(4)	0.040(6)	−0.008(4)	−0.014(5)	0.014(4)
W2	0.400(1)	0.1507(9)	0.945(2)	0.026(3)	0.016(5)	0.049(6)	0.040(6)	0.006(5)	−0.014(5)	−0.013(5)

Note: The thermal ellipsoid is given by $\exp[-2\pi^2(U_{11}h^2a^{*2} + U_{22}k^2b^{*2} + U_{33}l^2c^{*2} + 2U_{23}klb^*c^* + 2U_{13}hla^*c^* + 2U_{12}hka^*b^*)]$.
* Occupancy of this site is V = 0.62, As = 0.38.

TABLE 7. Bond valences and their sums (Σ) for each atom in fianelite

	Mn1	Mn2	V1	V2	W1	W2	Σ
O1	0.25	0.36		1.29		0.02	1.92
O2	0.37	0.33		1.35		0.05	2.10
O3			0.91	1.09	0.11 + 0.14		2.25
O4	0.42		1.49			0.10	2.01
O5		0.37		1.34	0.19	0.11	2.01
O6	0.34	0.37	1.29				2.00
O7	0.40	0.33	1.30				2.03
W1	0.32						0.32
W2		0.31					0.31
Σ	2.10	2.07	4.99	5.07			

Note: Bond valences were calculated using the formula and constants of Altermatt and Brown (1985). Hydrogen-bond valences were estimated using Figure 2 of Altermatt and Brown (1985).

and structure-refinement results are summarized in Table 4, and fractional atomic coordinates and displacement parameters are listed in Table 6.

The low chemical-analysis totals from the EMP suggest that fianelite contains H atoms. A difference-Fourier synthesis did not reveal any reasonable peak that could be interpreted as an H position. Two O atoms with very low empirical bond-valence sums (Table 7) were assigned to H_2O groups, labeled W1 and W2 (Table 6). These two O positions have significantly higher displacement parameters, as can be seen from Table 6. Geometrical considerations from the topology of the structure further support this interpretation (see below).

TABLE 8. Selected interatomic distances (Å) in fianelite

V1-O3	1.83(1)
V1-O4	1.657(9)
V1-O6	1.71(1)
V1-O7	1.70(1)
Mean	1.72
V2-O1	1.70(1)
V2-O2	1.680(9)
V2-O3	1.76(1)
V2-O5	1.68(1)
Mean	1.71
Mn1-O1	2.30(1)
Mn1-O2	2.16(1)
Mn1-O4	2.11(1)
Mn1-O6	2.20(1)
Mn1-O7	2.13(1)
Mn1-W1	2.21(1)
Mean	2.19
Mn2-O1	2.17(1)
Mn2-O2	2.20(1)
Mn2-O5	2.16(1)
Mn2-O6	2.16(1)
Mn2-O7	2.20(1)
Mn2-W2	2.22(1)
Mean	2.19
W1-O5	2.78(2)*
W1-O3′	2.93(1)*
W1-O7	2.95(2)**
W1-O3″	2.99(2)
W1-O4	3.02(2)**
W1-O1	3.20(1)**
W2-W1	3.20(2)
W2-O2′	2.97(2)**
W2-O4	2.99(1)*
W2-O5	2.99(2)
W2-O1′	3.02(2)**
W2-O2″	3.10(1)
W2-O1″	3.16(2)
W2-O6	3.19(2)**

* Bond across the cavity (indicated for bonds between H_2O group and O; see Fig. 5).

** Bond within the same octahedron (indicated for bonds between H_2O group and O).

TABLE 9. Selected interatomic angles (°) in fianelite

O3-V1-O4	109.3(5)	O1-V2-O2	110.9(5)
O3-V1-O6	104.5(5)	O1-V2-O3	108.2(5)
O3-V1-O7	107.2(5)	O1-V2-O5	112.2(5)
O4-V1-O6	112.8(5)	O2-V2-O3	106.7(5)
O4-V1-O7	111.3(5)	O2-V2-O5	113.3(5)
O6-V1-O7	111.3(5)	O3-V2-O5	105.1(4)
Mean	109.4	Mean	109.4
O1-Mn1-O2	90.0(4)	O1-Mn2-O5	96.7(4)
O1-Mn1-O6	85.3(4)	O1-Mn2-O6	103.5(4)
O1-Mn1-O7	80.2(4)	O1-Mn2-O7	81.6(4)
O1-Mn1-W1	90.3(4)	O1-Mn2-W2	87.1(5)
O2-Mn1-O4	91.2(3)	O2-Mn2-O5	91.5(4)
O2-Mn1-O6	82.4(4)	O2-Mn2-O6	82.3(4)
O2-Mn1-O7	87.9(4)	O2-Mn2-O7	93.8(4)
O4-Mn1-O6	91.9(4)	O2-Mn2-W2	84.6(4)
O4-Mn1-O7	102.8(4)	O5-Mn2-O6	87.9(4)
O4-Mn1-W1	88.9(4)	O5-Mn2-O7	83.7(4)
O6-Mn1-W1	104.1(4)	O6-Mn2-W2	93.4(4)
O7-Mn1-W1	85.8(5)	O7-Mn2-W2	94.7(4)
Mean	90.1	Mean	90.1
O3′-W1-O3″	75.8(4)	O1′-W2-O2′	61.8(4)
O3′-W1-O4	106.8(5)	O1′-W2-O2″	52.8(3)
O3″-W1-O4	167.9(5)	O1′-W2-O4	95.7(4)
O3′-W1-O5	57.1(4)	O1′-W2-O5	110.5(5)
O3″-W1-O5	78.5(4)	O1′-W2-W1	84.9(4)
O3′-W1-O7	123.6(6)	O2′-W2-O2″	111.4(5)
O3″-W1-O7	108.6(4)	O2′-W2-O4	148.6(6)
O3′-W1-W2	64.2(3)	O2″-W2-O4	60.1(3)
O3″-W1-W2	139.9(5)	O2′-W2-O5	138.7(5)
O4-W1-O5	111.4(5)	O2″-W2-O5	61.6(4)
O4-W1-O7	67.4(4)	O2′-W2-W1	90.1(4)
O4-W1-W2	112.0(4)	O2″-W2-W1	101.9(4)
O5-W1-O7	172.8(6)	O4-W2-O5	67.3(4)
O5-W1-W2	78.4(4)	O4-W2-W1	64.9(4)
O7-W1-W2	95.4(5)	O5-W2-W1	130.9(5)

STRUCTURE DESCRIPTION

Selected interatomic distances and angles are listed in Tables 8 and 9, respectively. The two average Mn-O distances, in comparison with the mean octahedral bond length reported in the literature for Mn^{2+}, preclude the presence of Mn in the trivalent oxidation state. The presence of tetrahedra and the tetrahedral dimensions are in agreement with the pentavalent oxidation state for V, which holds for the dominant ion in both tetrahedral site populations. The empirical bond valences estimated from the final refined structure (Table 7) also confirm the inferred cation oxidation states. The structure refinement revealed that As substitutes only for V2. The As content inferred by the structure analysis is 0.38 As pfu. Electron microprobe results for a zoned polycrystalline aggregate not submitted to single-crystal study suggest that As can be dominant (0.57 As pfu) on the V2 site.

In the structure of fianelite no closest-packed array of O atoms was observed. The polyhedral framework consists of octahedra and tetrahedra. The structural arrangement can be described in terms of octahedra forming zigzag chains subparallel to (101) and extending in the [$\bar{1}$01] direction. The octahedral chains are bound together by

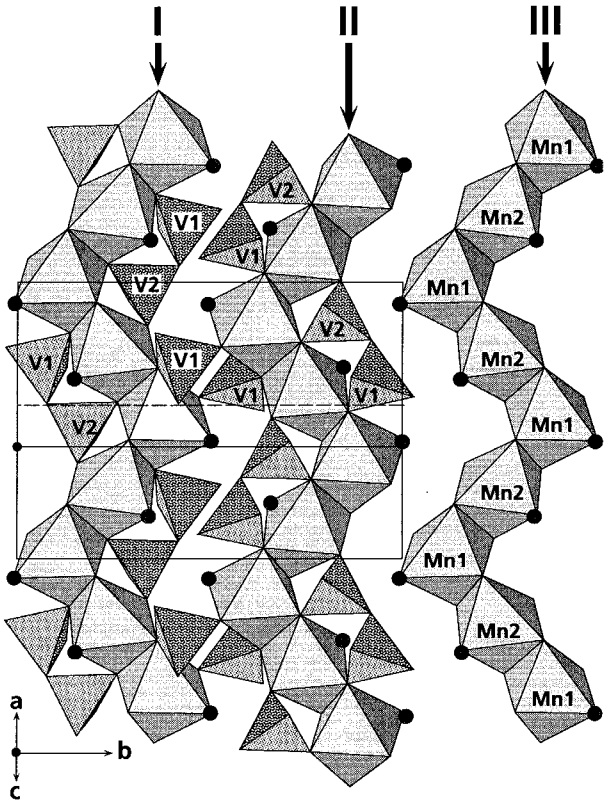

FIGURE 4. Orthographic projection of the octahedral chains on the (101) plane. The unit-cell outline is shown. All neighboring tetrahedra were removed from chain III. The tetrahedra that cross-link chains I and II are shown, along with the neighboring tetrahedra of chains I and II within the (101) plane.

pairs of tetrahedra (Fig. 4). Each pair of tetrahedra shares three O atoms with one octahedral chain, two O atoms with a second, and one O atom with a third. The polyhedral framework contains cavities that cross the whole structure along [001] (Fig. 5). The cavities are elongated along [130] and [1$\bar{3}$0]. The H_2O groups are located on the apices of the octahedra that point to these cavities. W2 forms weak hydrogen bonds with neighboring O atoms [smallest W-O distance: W2-O2 = 2.97(2) Å; Table 8]. W1 forms a stronger hydrogen bond with O5 at 2.78(2) Å; the other O atoms are at distances ≥2.93(1) Å. Analysis of a crystal of better quality, however, is necessary to understand fully the role of the H_2O groups in the structure of fianelite.

The only natural manganese vanadate described so far is reppiaite, $Mn_5^{2+}(VO_4)_2(OH)_4$ (Basso et al. 1992), a mineral structurally related to cornubite. A structural comparison of fianelite and other minerals with similar atomic proportions among the vanadates, arsenates, and phosphates (of which the crystal structures are known) did not reveal any close relationship. In particular, the chains of octahedra have no equivalent topology among these minerals. The minerals of the haidingerite group

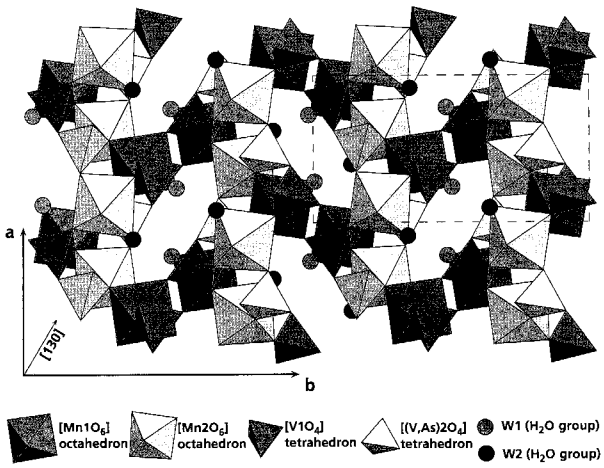

FIGURE 5. Orthographic projection of polyhedra in the fianelite structure along [001]. Dashed line indicates unit-cell outline.

[e.g., krautite, $Mn(AsO_3OH)\cdot H_2O$; haidingerite, $Ca(AsO_3OH)\cdot H_2O$] and the brushite group [e.g., fluckite, $CaMn(AsO_3OH)_2\cdot 2H_2O$] are characterized by a sheet topology of octahedra. In the minerals of the variscite group (e.g., variscite, $AlPO_4\cdot 2H_2O$), the octahedra are isolated.

ACKNOWLEDGMENTS

This study was supported by the Swiss National Funds for Scientific Research (grant no. 21-36495.92). The measurements on the CAD4 were made at the Laboratory for Crystallography, Department of Chemistry, University of Basel, and those on the Philips SEM 515 were made at the SEM-Laboratory, also at the University of Basel. We are grateful to S. Graeser, M. Zehnder, R. Guggenheim, H. Hänny, A. Edenharter, R. Gieré, M. Neuburger, D. Mathys, M. Braun, S. Schmidt, and many others for their help and constructive discussions. We thank T.S. Ercit and J. Grice (Ottawa) for helpful reviews of the manuscript.

REFERENCES CITED

Altermatt, D., and Brown, I.D. (1985) Bond-valence parameters obtained from a systematic analysis of the inorganic crystal structure database. Acta Crystallographica, B41, 244–248.

Altomare, A., Cascarano, G., Giacovazzo, G., Guagliardi, A., Burla, M.C., Polidori, G., and Camalli, M. (1994) SIR92: A program for automatic solution of crystal structures by direct methods. Journal of Applied Crystallography, 27, 435.

Bari, H., Cesbron, F., Permingeat, F., and Pillard, F. (1980) La fluckite, arséniate hydraté de calcium et manganèse $CaMnH_2(AsO_4)_2\cdot 2H_2O$, une nouvelle espèce minérale. Bulletin de la Société français de Minéralogie et de Cristallographie, 103, 122–128.

Basso, R. (1987) The crystal structure of palenzonaite, a new vanadate garnet from Val Graveglia (Northern Apennines, Italy). Neues Jahrbuch für Mineralogie Monatshefte, 3, 136–144.

Basso, R., Lucchetti, G., Zefiro, L., and Palenzona, A. (1992) Reppiaite, $Mn_5(OH)_4(VO_4)_2$, a new mineral from Val Graveglia (Northern Apennines, Italy). Zeitschrift für Kristallographie, 201, 223–234.

Baudin, T., Marquer, D., Barfety, J.-C., Kerchkove, C., and Persoz, F. (1995) A new stratigraphical interpretation of the Mesozoic cover of the Tambo and Suretta nappes: Evidence for early thin-skinned tectonics (Swiss Central Alps). Comptes Rendus de l'Académie des Sciences de Paris, Série IIa, 321, 401–408.

Beneke, K., and Lagaly, G. (1981) Krautite, $MnHAsO_4\cdot H_2O$: An intracrystalline reactive mineral. American Mineralogist, 66, 432–435.

Calleri, M., and Ferraris, G. (1967) Struttura della haidingerite: $CaH(AsO_4)\cdot H_2O$. Periodico di Mineralogia, 36, 1–23.

Carruthers, J.R., and Watkin, D.J. (1979) A weighting scheme for least-squares structure refinement. Acta Crystallographica, A35, 698–699.

Cassien, M., Herpin, P., and Permingeat, F. (1966) Structure cristalline de la haidingérite. Bulletin de la Société français de Minéralogie et de Cristallographie, 89, 18–22.

Catti, M., and Franchini-Angela, M. (1979) Krautite, $Mn(H_2O)(AsO_3OH)$: Crystal structure, hydrogen bonding and relations with haidingerite and pharmacolite. American Mineralogist, 64, 1248–1254.

Catti, M., Chiari, G., and Ferraris, G. (1980) Fluckite, $CaMn(HAsO_4)_2\cdot 2H_2O$, a structure related by pseudo-polytypism to krautite $MnHAsO_4\cdot H_2O$. Bulletin de la Société français de Minéralogie et de Cristallographie, 103, 129–134.

Cortesogno, L., Luchetti, G., and Penco, A.M. (1979) Le mineralizzazioni a manganese nei diaspri delle ofioliti liguri: Mineralogia e genesi. Rendiconti della Società Italiana di Mineralogia e Petrologia, 35, 151–197.

Fontan, F., Orliac, M., and Permingeat, F. (1975) La krautite $MnHAsO_4\cdot H_2O$, une nouvelle espèce minérale. Bulletin de la Société français de Minéralogie et de Cristallographie, 98, 78–84.

Geiger, T. (1948) Manganerz in den Radiolariten Graubündens. Beiträge zur Geologie der Schweiz, Geotechnische Serie, 27, 89 p.

Graeser, S., Schwander, H., and Suhner, B. (1984) Grischunit ($CaMn_2[AsO_4]_2$), eine neue Mineralart aus den Schweizer Alpen. Schweizerische Mineralogische und Petrographische Mitteilungen, 64, 1–10.

Graeser, S., Schwander, H., Bianchi, R., Pilati, T., and Gramaccioli, C.M. (1989) Geigerite, the Mn analogue of chudobaite: Its description and crystal structure. American Mineralogist, 74, 676–684.

Kniep, R., Mootz, D., and Vegas, A. (1977) Variscite. Acta Crystallographica, B33, 263–265.

Lucchetti, G., Penco, A.M., and Rinaldi, R. (1981) Saneroite, a new natural hydrated Mn-silicate. Neues Jahrbuch für Mineralogie Monatshefte, 4, 161–168.

Mandarino, J.A. (1976) The Gladstone-Dale relationship: Part I. Derivation of new constants. Canadian Mineralogist, 14, 498–502.

Schmid, S.M., Rück, P., and Schreurs, G. (1990) The significance of the Schams nappes for the reconstruction of the paleotectonic and orogenic evolution of the Penninic zone along the NFP-20 East traverse (Grisons, Eastern Switzerland). Mémoires de la Société Geologique de France, 156, 263–287.

Schreurs, G. (1991) Structural analysis of the Schams nappes and adjacent tectonic units in the Penninic zone (Grisons, SE-Switzerland). Ph.D. thesis, Mitteilungen aus dem geologischen Institut der eidgenossischen technischen Hochschule und der Universität Zürich, Neue Folge, 283, 204 p.

Stucky, K. (1960) Die Eisen- und Manganerze in der Trias des Val Ferrera. Beiträge zur Geologie der Schweiz, Geotechnische Serie, 37, 67 p.

Trümpy, R. (1980) Geology of Switzerland, a guide book: Part A. An outline of the geology of Switzerland, 104 p. Schweizerische geologische Kommission, Wepf, Basel.

Walker, N., and Stuart, D. (1983) An empirical method for correcting diffractometer data for absorption effects. Acta Crystallographica, A39, 158–166.

Watkin, D.J., Carruthers, R.J., and Betteridge, P. (1985) CRYSTALS. Chemical Crystallography Laboratory, Oxford, U.K.

Yvon, K., Jeitschko, W., and Parthé, E. (1977) LAZY PULVERIX, a computer program, for calculating X-ray and neutron diffraction powder patterns. Journal of Applied Crystallography, 10, 73–74.

Manuscript received October 10, 1995
Manuscript accepted May 13, 1996